ISSN 8756-6990, Optoelectronics, Instrumentation and Data Processing, 2023, Vol. 59, No. 5, pp. 612–619. © Allerton Press, Inc., 2023.
Russian Text © The Author(s), 2023, published in Avtometriya, 2023, Vol. 59, No. 5, pp. 91–99.

OPTICAL-PHYSICAL METHODS OF RESEARCH AND MEASUREMENT

Optimization of The Thickness of Single-Layer Antireflection SiO_2 Coating on a Silicon Photodiode Depending of the Characteristics of Incident Light

A. V. Timofeev[1*], A. I. Mil'shtein[1,2], and D. N. Grigor'ev[1,2,3]

[1] *Budker Institute of Nuclear Physics, Siberian Branch, Russian Academy of Sciences, Novosibirsk, 630090 Russia*

[2] *Novosibirsk State University, Novosibirsk, 630090 Russia*

[3] *Novosibirsk State Technical University, Novosibirsk, 630073 Russia*

Received February 6, 2023; revised March 30, 2023; accepted April 6, 2023

Abstract—Theoretical investigations of the dependence of the optimal thickness of a one-layer antireflection SiO_2 coating on a silicon photodiode on the characteristics of the light incident to the photodiode. It is shown that the optimal thickness of the one-layer antireflection SiO_2 coating for different angular distributions of intensity increases the quantum efficiency of the photodiode by up to 1.1 times in comparison with the classical one-layer antireflection coating with a thickness $\lambda/4n$, which is optimal in the case of the normal incidence of monochromatic light.

DOI: 10.3103/S8756699023050096

Keywords: *antireflection coating, photodiode, reflection coefficient*

INTRODUCTION

To increase the quantum efficiency of photodetectors, one uses various special antireflection coatings which make it possible to reduce the reflection coefficient up to the values close to several percents in a wide range of wavelengths and the normal incidence of light [1–11]. In the process of producing photodetectors, the operation of deposition of a special antireflection coating requires the use of additional equipment, which leads to complication of the technology of photodetector production. In some problems, special blooming is a redundant operation; therefore, with the purpose of making the technology of photodetector production cheaper and simpler, it is possible to use a layer of silicon dioxide whose deposition onto silicon is a standard operation when producing silicon photodetectors [12, 13] instead of depositing a special antireflection coating. To reduce the reflection coefficient, the necessary thickness of silicon dioxide for the normal or oblique incidence of a parallel beam of monochromatic light is calculated by using the formula [1]

$$d = \frac{\lambda(2l+1)}{4n\cos\theta}, \quad l = 0, 1, 2, 3, \ldots, \tag{1}$$

where λ is the wavelength of incident light, n is the refraction index of the one-layer antireflection coating, θ is the incidence angle relative to the photodiode's normal. In the simplest case for the normal incidence, $d = \lambda/4n$, which corresponds to the quarter-wave coating in optics. However, there are the problems in which light is not monochromatic and the incidence angle with respect to the photodetector varies within some angle interval; at that, the light intensity depends on the incidence angle. The examples of such problems are the cases when light is transmitted through optical or wavelength-shifting fibers [14–17]. In such cases, the angular and spectral distribution of the light incident to the photodetector is determined by the characteristics of the optical or wavelength-shifting

*E-mail: A.V.Timofeev@inp.nsk.su

fiber. Correspondingly, the optimal thickness of the antireflection coating depends on the light intensity distribution over angles and wavelengths; therefore, formula (1) cannot be applied.

The aim of this work is to calculate the optimal thickness of the SiO_2 layer for the case when the intensity of the light incident to the photodiode is bounded with respect to the maximum incident angle and is distributed according to the Lambert law or does not depend on the angle:

$$I(\lambda,\theta)=\begin{cases} I_0(\lambda)\cos\theta, & \theta\leqslant\theta_{\max};\\ 0, & \theta>\theta_{\max}, \end{cases} \tag{2}$$

$$I(\lambda,\theta)=\begin{cases} I_0(\lambda), & \theta\leqslant\theta_{\max};\\ 0, & \theta>\theta_{\max}, \end{cases} \tag{3}$$

where θ is the light incidence angle and $\theta_{\max}$ is the maximum angle with respect to the fiber axis.

CALCULATIONS

To determine the coefficient of reflection from the plane layer, the ratio of the amplitudes of the incident wave to that reflected from the air—silicon dioxide interface was calculated with consideration of reflection at the silicon dioxide—silicon interface. It should be noted that when solving the Maxwell equations, there is no necessity to take into account the effect of multiple reflection in the air and silicon dioxide, since it is already considered automatically. It follows from the boundary conditions that at $x=0$ and $x=d$, the tangential components of vectors **E** and **H** are continuous. Therefore, we can obtain the system of equations for the case of polarization of the wave perpendicular to the plane of incidence (the normally polarized wave, Fig. 1):

$$E_0+E_1=E_2+E_3, \tag{4}$$

$$\sqrt{\frac{\varepsilon_1}{\mu_1}}\,E_0\cos\theta_1-\sqrt{\frac{\varepsilon_1}{\mu_1}}\,E_1\cos\theta_1=\sqrt{\frac{\varepsilon_2}{\mu_2}}\,E_2\cos\theta_2-\sqrt{\frac{\varepsilon_2}{\mu_2}}\,\dot{E}_3\cos\theta_2, \tag{5}$$

$$E_2\mathbf{e}^{ik_2d\cos\theta_2}+E_3\mathbf{e}^{-ik_2d\cos\theta_2}=E_4\mathbf{e}^{ik_3d\cos\theta_3}, \tag{6}$$

$$\sqrt{\frac{\varepsilon_2}{\mu_2}}\,E_2\mathbf{e}^{ik_2d\cos\theta_2}\cos\theta_2-\sqrt{\frac{\varepsilon_2}{\mu_2}}\,E_3\mathbf{e}^{-ik_2d\cos\theta_2}\cos\theta_2 =\sqrt{\frac{\varepsilon_3}{\mu_3}}\,E_4\mathbf{e}^{ik_3d\cos\theta_3}\cos\theta_3, \tag{7}$$

where

$$k_i=\frac{2\pi\sqrt{\varepsilon_i\mu_i}}{\lambda}, \tag{8}$$

ε is the relative permittivity of the medium and μ is the relative magnetic permeability of the medium.

The solution of this system of equations has the form

$$A_E=\frac{E_1}{E_0}=\frac{a_{12}(1-Z_E)-(1+Z_E)}{a_{12}(1-Z_E)+(1+Z_E)}, \tag{9}$$

where

$$Z_E=\frac{1-a_{23}}{1+a_{23}}\mathbf{e}^{i2n_2\frac{2\pi d}{\lambda}\cos\theta_2},\quad a_{12}=\frac{\cos\theta_1}{\cos\theta_2}\sqrt{\frac{\varepsilon_1}{\mu_1}}\sqrt{\frac{\mu_2}{\varepsilon_2}},\quad a_{23}=\frac{\cos\theta_2}{\cos\theta_3}\sqrt{\frac{\varepsilon_2}{\mu_2}}\sqrt{\frac{\mu_3}{\varepsilon_3}}, \tag{10}$$

$$n_1\sin\theta_1=n_2\sin\theta_2=n_3\sin\theta_3,\quad n_1=\sqrt{\varepsilon_1\mu_1},\quad n_2=\sqrt{\varepsilon_2\mu_2},\quad n_3=\sqrt{\varepsilon_3\mu_3}\,. \tag{11}$$

For the case of polarization of the wave lying in the scattering plane (the wave with parallel polarization, Fig. 2), we get the following system of equations:

$$\sqrt{\frac{\varepsilon_1}{\mu_1}}\,E_0+\sqrt{\frac{\varepsilon_1}{\mu_1}}\,E_1=\sqrt{\frac{\varepsilon_2}{\mu_2}}\,E_2+\sqrt{\frac{\varepsilon_2}{\mu_2}}\,E_3, \tag{12}$$

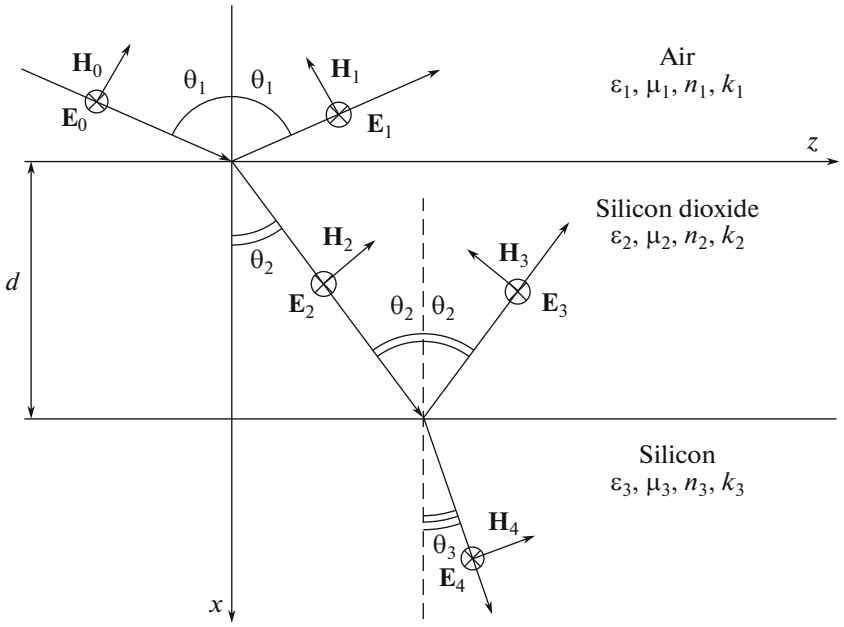

Fig. 1. Scheme of propagation of a normally polarized wave.

$$-E_0\cos\theta_1 + E_1\cos\theta_1 = -E_2\cos\theta_2 + E_3\cos\theta_2, \tag{13}$$

$$\sqrt{\frac{\varepsilon_2}{\mu_2}}\,E_2\mathbf{e}^{ik_2d\cos\theta_2} + \sqrt{\frac{\varepsilon_2}{\mu_2}}\,E_3\mathbf{e}^{-ik_2d\cos\theta_2} = \sqrt{\frac{\varepsilon_3}{\mu_3}}\,E_4\mathbf{e}^{ik_3d\cos\theta_3}, \tag{14}$$

$$-E_2\cos\theta_2\mathbf{e}^{ik_2d\cos\theta_2} + E_3\cos\theta_2\mathbf{e}^{-ik_2d\cos\theta_2} = -E_4\cos\theta_3\mathbf{e}^{ik_3d\cos\theta_3}. \tag{15}$$

The solution of this system has the form

$$A_M = \frac{E_1}{E_0} = \frac{b_{12}(1-Z_M)-(1+Z_M)}{b_{12}(1-Z_M)+(1+Z_M)}, \tag{16}$$

where

$$Z_M = \frac{1-b_{23}}{1+b_{23}}\mathbf{e}^{i2n_2\frac{2\pi d}{\lambda}\cos\theta_2}, \quad b_{12} = \frac{\cos\theta_1}{\cos\theta_2}\sqrt{\frac{\varepsilon_2}{\mu_2}}\sqrt{\frac{\mu_1}{\varepsilon_1}}, \quad b_{23} = \frac{\cos\theta_2}{\cos\theta_3}\sqrt{\frac{\varepsilon_3}{\mu_3}}\sqrt{\frac{\mu_2}{\varepsilon_2}}, \tag{17}$$

$$n_1\sin\theta_1 = n_2\sin\theta_2 = n_3\sin\theta_3, \quad n_1 = \sqrt{\varepsilon_1\mu_1}, \quad n_2 = \sqrt{\varepsilon_2\mu_2}, \quad n_3 = \sqrt{\varepsilon_3\mu_3}\,. \tag{18}$$

The dependencies obtained of the reflection coefficient on the light incidence angle for different polarizations coincide with the dependence obtained by using the matrix method in [1].

For a monochromatic light, the total reflection coefficient as a function of λ, d, and $\theta_{\max}$ is calculated by using the formula

$$R_L(\lambda,d,\theta_{\max}) = \frac{\int_0^{\theta_{\max}}(|A_E(\lambda,d,\theta_1)|^2 + |A_M(\lambda,d,\theta_1)|^2)I(\lambda,\theta_1)\sin\theta_1\,d\theta_1}{2\int_0^{\theta_{\max}} I(\lambda,\theta_1)\sin\theta_1\,d\theta_1}. \tag{19}$$

For the case with a nonmonochromatic light source, the reflection coefficient $R(\lambda,d,\theta_{\max})$ was additionally averaged over wavelengths:

$$R_{\text{tot}}(d,\theta_{\max}) = \frac{\int_{\lambda_{\min}}^{\lambda_{\max}} I_0(\lambda)R(\lambda,d,\theta_{\max})\,d\lambda}{\int_{\lambda_{\min}}^{\lambda_{\max}} I_0(\lambda)\,d\lambda}. \tag{20}$$

Since these integrals are not calculated analytically, the value of $R_{\text{tot}}(d,\theta_{\max})$ was analyzed numerically.

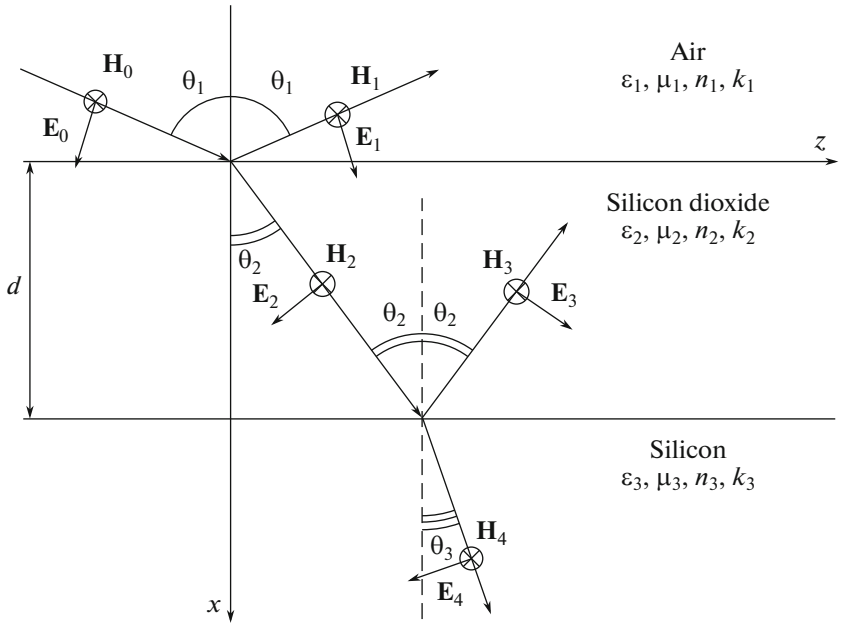

Fig. 2. Scheme of propagation of a parallel polarized wave.

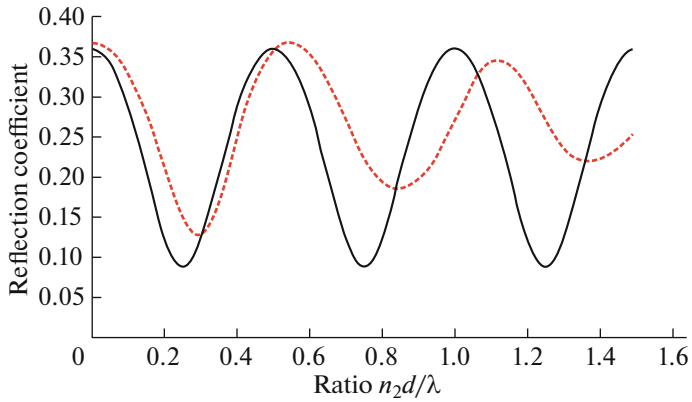

Fig. 3. Example of the dependence of the reflection coefficient of the value n_2d/λ for a Lambertian light source: solid curve $\theta_{\max} = 1°$, dotted $\theta_{\max} = 90°$ curve.

RESULTS

To determine the optimal ratio of the coating thickness to the wavelength, the dependence of the reflection coefficient on the value of n_2d/λ of the wave was calculated with a step 0.01.

Examples of the dependence of the reflection coefficient on the value of n_2d/λ are shown in Fig. 3. The positions of the first three minima of the reflection coefficient were determined numerically.

The optimal ratios n_2d/λ for the first three minima depending on the maximum angle are shown in Fig. 4.

At small light incidence angles, the results of calculation are expectedly in accordance with (1). It is seen that in the case of an uniform source (2) and large angles in Figs. 4b and 4c, the optima shift by nearly a quarter of wavelength, which corresponds to the maximum of reflection coefficient in the case of normal incidence.

The practical value of this calculation is demonstrated by the dependence of the ratio of the transmission coefficient at the optimal thickness to the transmission coefficient at the thicknesses obtained for

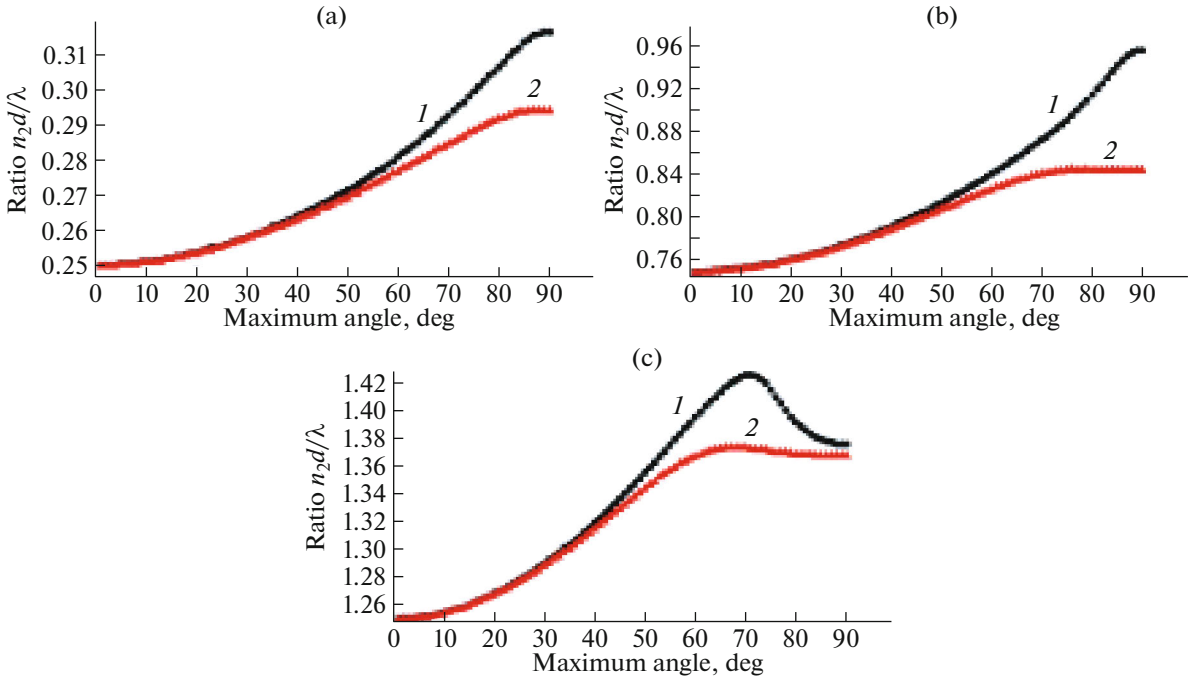

Fig. 4. Optimal ratio n_2d/λ for the first three minima: (a) the first minimum, (b) the second minimum, (c) the third minimum (curves *1*—incident light has an uniform angular distribution; curves *2*—incident light is distributed as a Lambert source).

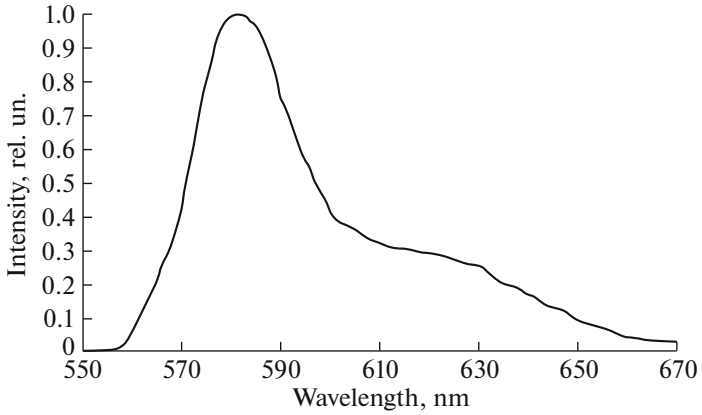

Fig. 5. Digitalized fluorescence spectrum of the wavelength-shifting O–2 fiber at a distance of 10 cm from the place of fluorescence.

the normal incidence (1) on $\theta_{\max}$:

$$Q = \frac{1 - R_{\text{tot}}(d_{\text{opt}}(\theta_{\max}), \theta_{\max})}{1 - R_{\text{tot}}(d_{\lambda/(4n_2)}, \theta_{\max})}, \tag{21}$$

where $d_{\text{opt}}(\theta_{\max})$ is the optimal thickness of silicon dioxide for the maximum angle $\theta_{\max}$ and $d_{\lambda/(4n_2)}$ is the silicon dioxide thickness obtained for the case of normal light incidence by using (1).

Calculation is performed for the wavelength shifting O-2 fiber produced by Kuraray, which was used in [15] with a PIN photodiode with an antireflection coating made of SiO_2. In the calculations, the fluorescence spectrum of the wavelength shifting fiber O-2 shown in Fig. 5 [18] was used. In the scientific literature [19–24], the spread of the values of refraction coefficients of silicon dioxide and silicon is about 1%; therefore, for the maximum of fluorescence of the wavelength shifting fiber O-2, we used the values 1.47 and 3.99, respectively. The imaginary part of permittivity was not considered, since it

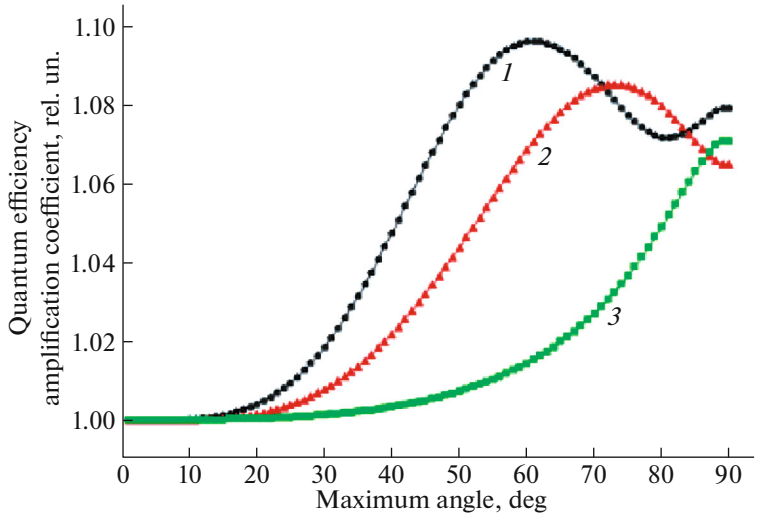

Fig. 6. Example of the dependence of the coefficient of quantum efficiency amplification of diode calculated by using (21). Denotations: curve *1*—3rd minimum, curve *2*—2nd minimum, curve *3*—1st minimum.

is very small. The dependence of the relative permittivity on the wavelength was not considered, since in the range of the fluorescence spectrum of the wavelength shifting fiber O-2, its value is insignificant. The relative magnetic permeability was assumed to be 1.

As an example, Fig. 6 shows the diode's quantum efficiency amplification coefficient for the light with the spectrum of the wavelength shifting fiber at a length of 10 cm (see Fig. 5) and an intensity uniformly distributed over angles (3).

The results shows that the coating with a thickness obtained by using (1) is optimal at the angles smaller than 30°. At the angles larger than 30°, the above calculation makes it possible to increase the quantum efficiency by the value from 1.02 to 1.10 times depending on the characteristics of the light incident to the photodiode.

CONCLUSIONS

The calculations of the optimal thickness of the one-layer antireflection coating of SiO_2 at a silicon photodiode are performed for the cases when the light incidence angle to the photodiode is bounded and its intensity is either distributed according to the Lambert law or does not depend on the angle. Application of the coating thickness calculated by using (1) can lead to a reduction of the photodiode quantum efficiency by 1.1 times as compared with the thickness calculated by using (20). The results can be used when designing photodiodes for their application in the detectors based on fiber optics or in scintillators.

FUNDING

This work was supported by ongoing institutional funding. No additional grants to carry out or direct this particular research were obtained.

CONFLICT OF INTEREST

The authors of this work declare that they have no conflicts of interest.

REFERENCES

1. E. S. Putilin, *Optical Coatings: Textbook* (S.-Peterb. Gos. Univ. ITMO, St. Petersburg, 2010).
2. A. V. Ershov and A. I. Mashin, *Multilayer Optical Coatings: Design, Materials, Peculiarities of Manufacturing Technology by the Electron-Beam Evaporation* (Nizhegorodsk. Gos. Univ., Nizhny Novgorod, 2006).
3. B. K. Ghosh, K. T. Tze Kin, and S. S. Mohd Zainal, "Different materials coating effect on responsivity of Si UV photo detector," in *2013 IEEE Conf. on Clean Energy and Technology (CEAT), Langkawi, Malaysia, 2013* (IEEE, 2013), pp. 446–449. https://doi.org/10.1109/ceat.2013.6775673
4. S. W. Glunz and F. Feldmann, "SiO_2 surface passivation layers—A key technology for silicon solar cells," Sol. Energy Mater. Sol. Cells **185**, 260–269 (2018). https://doi.org/10.1016/j.solmat.2018.04.029
5. A. V. Malevskaya, Yu. M. Zadiranov, A. A. Blokhin, and V. M. Andreev, "Studying the formation of antireflection coatings on multijunction solar cells," Tech. Phys. Lett. **45**, 1024–1026 (2019). https://doi.org/10.1134/S1063785019100262
6. S. Kh. Suleimanov, V. G. Dyskin, M. U. Dzhanklych, and N. A. Kulagina, "Effective antireflection coating based on TiO_2–SiO_2 mixture for solar cells," Tech. Phys. Lett. **39**, 305–307 (2013). https://doi.org/10.1134/S1063785013030267
7. F. V. Khoa, P. T. Ngo, and L. A. Gubanova, "Broadband antireflective coating by the method of molecular layer deposition," Izv. Vyssh. Uchebn. Zaved., Priborostr. **61**, 336–341 (2018). https://doi.org/10.17586/0021-3454-2018-61-4-336-341
8. V. V. Gavrushko and V. A. Lastkin, "Broadband silicon photodiode," Vestn. Novgorodsk. Gos. Univ., No. 81, 53–55 (2014). https://cyberleninka.ru/article/n/shirokodiapazonnyy-kremnievyy-fotodiod. Cited February 6, 2023.
9. A. K. Budtolaev, G. V. Liberova, and V. I. Khizhnyak, "Increasing the sensitivity of silicon p–i–n-photodiodes to the 1.06 mm radiation," Prikl. Fiz., No. 5, 47–49 (2018). https://applphys.orion-ir.ru/appl-18/18-5/PF-18-5-47.pdf. Cited February 6, 2023.
10. S. C. Lee, H. B. Jeon, K. H. Kang, H. Park, D. H. Lee, M. W. Lee, and K. S. Park, "Photo-responses of silicon photodiodes with different ARC thicknesses for scintillators," J. Korean Phys. Soc. **75**, 1038–1042 (2019). https://doi.org/10.3938/jkps.75.1038
11. M. Zumuukhorol, Z. Khurelbaatar, J.-H. Kim, K.-H. Shim, S.-N. Lee, S.-J. Leem, and Ch.-J. Choi, "Effect of a SiO_2 anti-reflection layer on the optoelectronic properties of germanium metal-semiconductor-metal photodetectors," J. Semicond. Technol. Sci. **17**, 483-491 (2017). https://doi.org/10.5573/jsts.2017.17.4.483
12. C. G. Kang, A. H. Park, H. K. Cha, J. H. Ha, N.-H. Lee, Yo. S. Kim, J.-H. Oh, J. M. Park, S. M. Kim, S.-J. Lee, and H. S. Kim, "In-house fabricated Si PIN diode with Al_2O_3 anti-reflection layer for radiation detectors," in *2017 IEEE Nuclear Science Symp. and Medical Imaging Conf. (NSS/MIC), Atlanta, 2017* (IEEE, 2017), pp. 1–3. https://doi.org/10.1109/nssmic.2017.8532610
13. B. G. Streetman and S. K. Banerje, *Solid State Electronic Devices* (Pearson, Boston). https://ftehrani.profile.semnan.ac.ir/downloads/file/221. Cited February 6, 2023.
14. Yu. N. Kharzheev, "Scintillation counters in modern high-energy physics experiments," Phys. Part. Nucl. **46**, 678–728 (2015). https://doi.org/10.1134/S1063779615040048
15. S. S. Afanasenko, R. R. Akhmetshin, D. N. Grigoriev, V. F. Kazanin, V. V. Porosev, A. V. Timofeev, and R. I. Shcherbakov, "Hard gamma quantum flow detector with minimized image noise and improved registration efficiency," Optoelectron., Instrum. Data Process. **57**, 185–194 (2021). https://doi.org/10.3103/S8756699021020023
16. F. Rêgo and L. Peralta, "Si-PIN photodiode readout for a scintillating optical fiber dosimeter," Radiat. Meas. **47**, 947–950 (2012). https://doi.org/10.1016/j.radmeas.2012.07.019
17. A. R. F. Barroso and J. Johnson, "Optical wireless communications omnidirectional receivers for vehicular communications," Int. J. Electron. Commun. **79**, 102–109 (2017). https://doi.org/10.1016/j.aeue.2017.05.042
18. Kuraray Co., Ltd., Wavelength Shifting Fibers. http://kuraraypsf.jp/psf/ws.html. Cited February 6, 2023.
19. L. Gao, F. Lemarchand, and M. Lequime, "Refractive index determination of SiO_2 layer in the UV/Vis/NIR range: spectrophotometric reverse engineering on single and bi-layer designs," J. Eur. Opt. Soc.: Rapid Publ. **8**, 13010 (2013). https://doi.org/10.2971/jeos.2013.13010
20. Yu. Jiang, H. Liu, L. Wang, D. Liu, C. Jiang, X. Cheng, Ya. Yang, and Yi. Ji, "Optical and interfacial layer properties of SiO_2 films deposited on different substrates," Appl. Opt. **53**, A83–A87 (2014). https://doi.org/10.1364/ao.53.000a83

21. C. M. Herzinger, B. Johs, W. A. McGahan, J. A. Woollam, and W. Paulson, "Ellipsometric determination of optical constants for silicon and thermally grown silicon dioxide via a multi-sample, multi-wavelength, multi-angle investigation," J. Appl. Phys. **83**, 3323–3336 (1998). https://doi.org/10.1063/1.367101
22. G. E. Jellison Jr., "Optical functions of silicon determined by two-channel polarization modulation ellipsometry," Opt. Mater. **1**, 41–47 (1992). https://doi.org/10.1016/0925-3467(92)90015-f
23. J. Šik, J. Hora, and J. Humlíček, "Optical functions of silicon at high temperatures," J. Appl. Phys. **84**, 6291–6298 (1998). https://doi.org/10.1063/1.368951
24. D. E. Aspnes and A. A. Studna, "Dielectric functions and optical parameters of Si, Ge, GaP, GaAs, GaSb, InP, InAs, and InSb from 1.5 to 6.0 eV," Phys. Rev. B **27**, 985–1009 (1983). https://doi.org/10.1103/physrevb.27.985

Translated by E. Smintova